Author Manuscript

Author Manuscript

Author Manuscript

Author Manuscript

HHS Public Access

Author manuscript

Atmos Environ (1994). Author manuscript; available in PMC 2021 March 01.

Published in final edited form as:

Atmos Environ (1994). 2020 March 1; 224: . doi:10.1016/j.atmosenv.2020.117292.

Use of low-cost PM monitors and a multi-wavelength aethalometer to characterize $PM_{2.5}$ in the Yakama Nation Reservation

Orly Stampfer[a,*], **Elena Austin**[a], **Terry Ganuelas**[b], **Tremain Fiander**[b], **Edmund Seto**[a], **Catherine Karr**[a]

[a]University of Washington Department of Environmental and Occupational Health Sciences, 4225 Roosevelt Way NE, STE 301 Seattle, WA 98105.

[b]Yakama Nation Environmental Management Program, P.O. Box 151 Toppenish, WA 98948.

Abstract

Rural lower Yakima Valley, Washington is home to the reservation of the Confederated Tribes and Bands of the Yakama Nation, and is a major agricultural region. Episodic poor air quality impacts this area, reflecting sources of particulate matter with a diameter of less than 2.5 micrometers ($PM_{2.5}$) that include residential wood smoke, agricultural biomass burning and other emissions, truck traffic, backyard burning, and wildfire smoke. University of Washington partnered with the Yakama Nation Environmental Management Program to investigate characteristics of $PM_{2.5}$ using 9 months of data from a combination of low-cost optical particle counters and a 5-wavelength aethalometer (MA200 Aethlabs) over 4 seasons and an episode of summer wildfire smoke. The greatest percentage of hours sampled with $PM_{2.5}$ >12 μg/m^3 occurred during the wildfire smoke episode (59%), followed by fall (23%) and then winter (21%). Mean (SD) values of Delta-C (μg/m^3), which has been posited as an indicator of wood smoke, and determined as the mass absorbance difference at 375-880nm, were: summer – wildfire smoke 0.34 (0.52), winter 0.27 (0.32), fall 0.10 (0.22), spring 0.05 (0.11), and summer – no wildfire smoke 0.04 (0.14). Mean (95% confidence interval) values of the absorption Ångström exponent, an indicator of the wavelength dependence of the aerosol, were: winter 1.5 (1.2-1.8), summer – wildfire smoke 1.4 (1.0-1.8), fall 1.3 (1.1-1.4), spring 1.2 (1.1-1.4), and summer – no wildfire smoke 1.2 (1.0-1.3). The trends in Delta-C and absorption Ångström exponents are consistent with expectations that a higher value reflects more biomass burning. These results suggest that biomass burning is an important contributor to $PM_{2.5}$ in the wintertime, and emissions associated with diesel and soot are important contributors in the fall; however, the variety of emissions sources and combustion conditions present in this region may limit the utility of traditional interpretations of aethalometer data. Further understanding of how to interpret aethalometer data in regions with complex

[*]Corresponding author: ostamp@uw.edu, 206-221-6156, 4225 Roosevelt Way NE, STE 301, Seattle, WA 98105.

Publisher's Disclaimer: This is a PDF file of an unedited manuscript that has been accepted for publication. As a service to our customers we are providing this early version of the manuscript. The manuscript will undergo copyediting, typesetting, and review of the resulting proof before it is published in its final form. Please note that during the production process errors may be discovered which could affect the content, and all legal disclaimers that apply to the journal pertain.

Declaration of interests

The authors declare that they have no known competing financial interests or personal relationships that could have appeared to influence the work reported in this paper.

Author Manuscript Author Manuscript Author Manuscript Author Manuscript

emissions would contribute to much-needed research in communities impacted by air pollution from agricultural as well as residential sources of combustion.

Keywords

biomass burning; aethalometer; low-cost sensor; $PM_{2.5}$; rural; agricultural

1. Background

1.1 Study motivation

Rural lower Yakima Valley, Washington is home to the reservation of the Confederated Tribes and Bands of the Yakama Nation, and is a major agricultural region. In 2013 through 2016, Yakima County had the greatest percentage of monitored days per year with $PM_{2.5}$ over 35 μg/m^3 in WA (Washington Tracking network). Residential wood smoke is felt to be a major contributor (Pruitt 2014; VanderSchelden et al, 2017), although local sources include agricultural biomass burning, wildfire smoke, emissions associated with truck traffic, other agricultural emissions, and backyard burning.

High exposure to wood smoke is associated with respiratory issues, including asthma and lower respiratory tract infections (Noonan and Balmes, 2010). Factors influencing pediatric asthma and lower respiratory tract infections in rural settings are under-studied (Estrada and Ownby, 2017). Wood smoke is of even greater concern during the late fall and winter months when weather inversions are common, trapping air pollution in the valley. Due to stagnant atmospheric conditions common in the wintertime in Yakima Valley, the county (for its jurisdiction) and Yakama Nation and EPA (for the Yakama Reservation) issue bans on burning.

It remains a research challenge to understand $PM_{2.5}$ in rural settings given the sparseness of regulatory monitoring. Low-cost air monitors estimating $PM_{2.5}$ concentrations are useful in providing greater spatial resolution in time-resolved $PM_{2.5}$ levels (Zikova et al, 2017; Morawska et al 2018). However, their accuracy varies by season (Sayahi, Butterfield, & Kelly, 2019) and PM concentration, and calibration is necessary especially at higher PM levels (Kelly et al, 2017). Low-cost PM monitors cannot distinguish between PM originating from residential wood smoke versus other PM sources. However, this information is important for developing interventions to mitigate emissions. A multi-wavelength aethalometer can complement low-cost PM monitors by providing information that may be used to address PM sources.

As part of the US EPA Monitoring for Communities Program, the University of Washington partnered with the Yakama Nation Environmental Management Program to investigate characteristics of local $PM_{2.5}$ using a combination of low-cost PM monitors, a regulatory $PM_{2.5}$ monitor, and a 5-wavelength aethalometer. We were particularly interested in the application of the aethalometer in distinguishing wood smoke in this region. This study used a combination of 9 months of $PM_{2.5}$, Delta-C, and absorption Ångström exponent data over 4 seasons, including a period of wildfire smoke, to further understand contributions to $PM_{2.5}$

Author Manuscript Author Manuscript Author Manuscript Author Manuscript

in this highly impacted, rural area, and to investigate the utility of Delta-C and Ångström exponent data in identifying source contributions in this region.

2. Methods

2.1 Sampling location

Data were collected at two Yakama Nation air monitoring sites: one in Toppenish, Washington from late fall 2017 to mid-summer 2018, and another in Harrah, Washington from mid-summer 2018 to mid-fall 2018. The Toppenish site is located near a high school, at the end of a residential area and near agricultural fields, an industrial area, and a major roadway (Highway 97). This air monitoring site contains a low-cost monitor and the EPA-recognized federal equivalent method (FEM) beta attenuation monitor (BAM) (EPA site ID 53-077-0015). The BAM measures an hourly average of $PM_{2.5}$ concentration. A second low-cost monitor was placed at the Harrah site about 11 miles west, located near an elementary school, in a heavy agricultural region, away from major highways. This second site was chosen due to interest in capturing emissions more specifically related to agriculture. This site was previously a tribal air monitoring site (inactive EPA site ID 53-077-0017).

2.2 Particulate air monitoring instruments

The low-cost air monitors (cost of components $1,500-$2,000) were designed and assembled in-house at University of Washington for use in prior studies. Two optical particle sensors (Plantower PMSA003) report instantaneous measures of particle counts every two to three minutes, with the following size cut-points: 0.3, 0.5, 1, 2.5, 5, and 10 micrometers. Additionally, the Plantower provides estimates of mass concentrations for PM_1, $PM_{2.5}$, and PM_{10}. The Plantower PMSA003 reports two sets of mass concentrations, CF=1 which is intended for factory calibrations, and ATM which is intended for ambient measurements. This study used the ATM $PM_{2.5}$ mass concentration values. The low-cost monitor also includes temperature and relative humidity (RH) sensors (Honeywell HIH6130).

Yakama Nation owns and operates the BAM, in collaboration with the WA Department of Ecology. The BAM measures aerosol sample $PM_{2.5}$ mass and reports hourly data. Hourly data was retrieved from the Washington State Department of Ecology's Air Quality Monitoring Website (Washington State Department of Ecology). BAM hourly $PM_{2.5}$ data was used to calibrate the low-cost monitor ATM $PM_{2.5}$ mass concentration data as described in section 2.5.

The other monitor utilized was a 5-wavelength aethalometer: the microAeth® MA200 (AethLabs) (2017 price <$10,000) which calculates particle mass every 1-minute at the following wavelengths: 880, 625, 528, 470, and 375 nm. The mass of particles that absorb light in the infrared (IR) range (880 nm) is considered to represent black carbon (BC) (Kirchstetter et al, 2004). The mass of particles that absorb light in the ultraviolet (UV) range (375 nm) is considered to represent brown carbon (BrC), which includes particles emitted by biomass burning (Laskin, Laskin, & Nizkorodov, 2015), such as wood smoke, tobacco, and agricultural burning. The PFTE filter automatically advances when it is saturated, and the filter cartridge was replaced as needed. The flow set point was 100 ml/min

Author Manuscript Author Manuscript Author Manuscript Author Manuscript

and the attenuation threshold was set to 50%. The first 30 minutes of measurements after a filter cartridge change were removed to mitigate estimates influenced by the instrument warming up. Optimized Noise Reduction Averaging was applied for every 5% change in the attenuation value for each channel, as described by Hagler et al (2011). Data was averaged by hour. The aethalometer also includes temperature and RH sensors.

2.3 Sampling timeframe

During the study period, Yakima Valley was highly impacted by summertime wildfire smoke from wildfires in Washington, nearby states, and British Columbia. The study aethalometer was co-located at both sites, with data divided into 5 time periods: winter (12/21/17-3/20/18, Toppenish), spring (3/21/18-6/20/18, Toppenish), summer wildfire smoke (8/1/18-9/9/18, Harrah), summer no wildfire smoke (6/21/18-7/31/18 and 9/10/18-9/21/18, Harrah), and fall (9/22/18-11/29/18, Harrah). Technical and site-based challenges interrupted data collection at several points (Figure 1).

Aethalometer data is available each month from January to October 2018, missing several days intermittently. The aethalometer data from most of July is not included in this study because the aethalometer was moved from Toppenish to Harrah on 7/25. BAM data is available from December 2017 to November 2018, missing nearly all of February and several days in June. Data from the low-cost monitor in Toppenish is available for December 2017 to March 2018 (missing several weeks in January and March), May to June 2018, and September to November 2018. Data from the low-cost monitor in Harrah is available from March to November 2018, missing several days at the end of July.

2.4 Absorption Ångström exponent

Absorption is denoted by b_{abs} (m^{-1}) and is specific to each wavelength. To convert b_{abs} to mass, the aethalometer uses mass absorption efficiency values denoted by σ (m^2g^{-1}) empirically derived by the manufacturer (AethLabs, San Francisco). Mass absorption efficiency values used for each wavelength of the MA200 are available in the supplementary information (SI) Table 1. Using these mass absorption efficiency values, b_{abs} can be back-calculated from the mass at each wavelength using the following equation:

$$b_{abs} = mass \times \sigma$$

The wavelength dependence of b_{abs} changes with aerosol composition, and can be described using the absorption Ångström exponent, denoted by α. Using α to describe wavelength dependence facilitates comparison between different studies using aethalometers (Sandradewi et al, 2008). In general, α has been observed to increase with more biomass burning (Kirchstetter et al, 2004; Zotter et al, 2017; Sandradewi et al, 2008).

Ångström exponent values (α) were derived from linear regression parameters of b_{abs} by wavelength (λ) on a log-log scale, using the following equation:

$$\ln(b_{abs}) = -\alpha \times \ln(\lambda) + b$$

Author Manuscript Author Manuscript Author Manuscript Author Manuscript

Wavelength dependence (b_{abs} vs. λ) was plotted with a power law fit using the parameters a and b calculated from the regression in the previous equation. The power law fit is shown in the following equation:

$$b_{abs} = e^{b} \times \lambda^{-\alpha}$$

2.5 Delta-C

Delta-C, the absorbance difference at 375nm-880nm, was used as a biomass burning indicator. Delta-C has been used as an indicator for residential wood smoke (Wang et al, 2011a; Wang et al, 2012a; Sandradewi et al, 2008; Zhang et al, 2017; Sofowote et al, 2014; Crilley et al, 2015), forest fires (Wang et al, 2011a; Wang et al, 2010; Landis et al, 2017; Kimbrough et al, 2015), and other biomass burning and fireworks (Wang et al, 2011b; Kirchstetter et al, 2004). Delta-C has also been used to estimate the relative contribution of wood smoke to $PM_{2.5}$ (Wang et al, 2011a; Wang et al, 2012a).

2.6 Calibration of the low-cost monitor

Numerous studies have documented the importance of accounting for relative humidity in calibrating low-cost PM sensors with reference PM instrument measures, and that the relationship between light scattering and relative humidity is non-linear (Liu et al, 2019; Chakrabarti et al, 2004; Jayaratne et al, 2018; Sioutas et al, 2000; Day et al, 2000). The Plantower sensor response exponentially increases at RH levels above 78% (Jayaratne et al, 2018). One challenge of applying previous calibration methodology is that different studies involve different particle composition, which affects particle light scattering, as well as varying RH. Not all sensors respond the same, and thus evaluations of, for example, Nova (Liu et al, 2019) and personal DataRAM (Chakrabarti et al, 2004), may not be applicable to calibration of the Plantower. Selection of the reference instrument may also influence calibration. Jayaratne, et al based calibration of the Plantower on the TEOM (Jayaratne et al, 2018), while we used the BAM. Choice of RH measurement could also influence the calibration. Jayaratne, et al relied upon the reference monitoring site's RH measurement (Jayaratne et al, 2018), while Liu et al (2019) and our study relied upon an RH sensor inside of the low-cost monitor enclosure. This RH measurement may be different from ambient air RH. Generally, our approach to calibration is consistent with these previous studies in that we rely upon empirical co-location data with reference instrumentation, measurement of RH as a potential influence on the relationship between low-cost sensor response and particle mass concentrations, and a calibration model that allows for non-linear exponential response to increasing RH.

One low-cost monitor was co-located with the BAM, running intermittently between fall 2017 and fall 2018 at the Toppenish site for PM monitor calibration. Seasonal (winter, spring, summer, and fall) calibration equations were calculated by conducting multiple linear regressions between the hourly low-cost and BAM $PM_{2.5}$ mass concentration data. Summer wildfire and no wildfire periods were combined into a single summer season for the calibration model to include more data in the regression. All of the available co-located BAM and Toppenish low-cost monitor data were included in the calibration models. Each

Author Manuscript Author Manuscript Author Manuscript Author Manuscript

regression included RH, RH^2, and temperature as co-variates to account for the potential impact of RH and temperature on sensor accuracy (Jayaratne et al, 2014; Chakrabarti et al, 2004; Zheng et al, 2018; Liu et al, 2019). RH and temperature data came from sensors within the low-cost monitor. Low-cost monitor temperature and RH were compared to each other and to the BAM and Washington State University's AgWeatherNet Toppenish Station (AgWeatherNet) to confirm it is appropriate to use within-monitor temperature and RH data for the calibration. The model used is shown in the following expression:

$$BAM\ PM_{2.5} \sim low\ cost\ PM_{2.5} + RH + RH^2 + temperature$$

Parameters calculated for each variable from the multiple linear regressions were used to establish calibrated $PM_{2.5}$ values, using the following equation:

$$Calibrated\ PM_{2.5} = \beta_0 + \beta_1 \times low\ cost\ PM_{2.5} + \beta_2 \times RH + \beta_3 \times RH^2 + \beta_4 \times temperature$$

Where β_0 is the intercept, β_1 is the coefficient for the low-cost $PM_{2.5}$, β_2 is the coefficient for RH, β_3 is the coefficient for RH squared, and β_4 is the coefficient for temperature. The seasonal calibration models were used to adjust data by season from the low-cost monitor located in Harrah.

The two low-cost monitors were co-located in Seattle, WA from 7/10/17 to 7/13/17 for a total of 69 hours. We assessed the correlation and mean absolute difference of hourly $PM_{2.5}$ mass concentration data from these two monitors to confirm that it is appropriate to use a calibration equation from the monitor in Toppenish and apply it to the monitor in Harrah.

2.7 Analyses

For each time period when both aethalometer and co-located $PM_{2.5}$ data were available, hourly mean $PM_{2.5}$, Delta-C, IR, and Delta-C:$PM_{2.5}$ were calculated. Temperature from the BAM and RH from the AgWeatherNet Toppenish station were reported to provide context for seasonal weather differences. For Delta-C:$PM_{2.5}$ only, $PM_{2.5}$ <1 μg/m^3 (7.7% of sampled hours) were excluded to avoid spuriously high or negative ratio values that occur with noise in the Delta-C data and almost zero $PM_{2.5}$ mass values. This ratio used Harrah low-cost monitor $PM_{2.5}$ data in the summer and fall, and Toppenish BAM data in the winter and spring. A non-parametric Kruskal-Wallis test (Kruskal and Wallis, 1952) followed by a Dunn multiple-comparison test using bonferroni p-value adjustment (Dunn, 1964; Pohlert, 2014) was used to assess statistical significance of seasonal differences in mean $PM_{2.5}$, Delta-C, IR, and Delta-C:$PM_{2.5}$. The Dunn test was repeated with each season treated as the control group to identify pairwise differences between season.

Wavelength dependence was plotted and α (375-880nm) values were calculated by season. Diurnal patterns of $PM_{2.5}$, Delta-C, and α values were assessed using boxplots for each hour. Delta-C, $PM_{2.5}$, and α values were also compared by season between weekends and weekdays, with non-parametric Kruskal-Wallis tests comparing weekends vs. weekdays within each season. The number and percentage of hours per season with $PM_{2.5}$ >12 μg/m^3 were calculated, as well as the α values for those peak hours.

Author Manuscript Author Manuscript Author Manuscript Author Manuscript

All of the available aethalometer data were analyzed to assess statistical significance of seasonal differences in α values using a non-parametric Kruskal-Wallis test followed by a Dunn multiple-comparison test using bonferroni p-value adjustment, with the Dunn test repeated with each season treated as the control group as described above. All of the available $PM_{2.5}$ data were used to compare seasonal $PM_{2.5}$ concentrations between Toppenish and Harrah.

Negative PM and aethalometer data were included in these analyses. Negative BAM $PM_{2.5}$ data are due to expected instrument noise (Schulte, 2017), negative low-cost monitor $PM_{2.5}$ data are due to the application of the calibration equation, and negative aethalometer data are due to either measurement error or volatility of species in the aerosol sample (Wang et al, 2011b). For both Toppenish and Harrah, the two Plantowers in each monitor were compared, and failed Plantowers (those with readings >3000 $\mu g/m^3$) were not used. During the study period, one Plantower in each monitor failed. Data from the other Plantower in each monitor were used. During the fall season, the remaining Plantower in Harrah had 81 data points (prior to averaging by hour) with $PM_{2.5}$ readings >3000 $\mu g/m^3$. These data were excluded. All analyses were completed using R version 3.5.1 (2018-07-02).

3. Results and Discussion

This paper describes one of the first applications of seasonal PM and BC monitoring in rural Yakima Valley, based on a combination of low-cost PM monitors, regulatory PM monitoring, and a multi-wavelength aethalometer. In conducting this study, we demonstrated the usefulness of low-cost monitor calibration with the local FEM BAM, and combined use of calibrated PM concentrations with information on Delta-C and absorption Ångström exponent to understand how biomass burning, wildfire smoke, and other sources of $PM_{2.5}$ and BC impact the Yakama Reservation airshed.

3.1 Low-cost monitor calibration

During the pre-study co-location in Seattle, WA, Pearson's correlation for hourly average $PM_{2.5}$ ($\mu g/m^3$) from the Plantowers used in this study was 0.94 (95% confidence interval (CI) 0.90-0.96). The mean absolute difference was 0.08 $\mu g/m^3$. The Pearson's correlation for temperature and RH were both 0.99 (95% CI 0.99-1.0).

During the study period, Toppenish low-cost monitor temperature and RH differed from BAM temperature and AgWeatherNet RH (Table 1). Low-cost monitor temperature tended to be higher than BAM temperature, and low-cost monitor RH tended to be lower than BAM RH. This is expected as the low-cost monitor temperature and RH sensors are within the monitor enclosure, resulting in warmer and drier conditions.

For the seasonal calibration equations, summer and fall R^2 exceeded spring and winter (Figure 2). The range of β_1 values ($PM_{2.5}$ slope) was 0.45 to 0.58 (SI Table 2). In each season, the calibration equation resulted in values closer to the 1-1 line, as compared to the raw data (Figure 2).

Author Manuscript Author Manuscript Author Manuscript Author Manuscript

The relationships appear to be non-linear at $PM_{2.5}$ values above about 25 μg/m^3. These values comprise 10.6% of fall $PM_{2.3}$ measurements, 1.9% of winter, 0% of spring, and 5.3% of summer. We tested alternative calibration equations for fall using terms for $PM_{2.5}^2$, $PM_{2.5}^3$, and $PM_{2.5}^4$, and found that the mean absolute difference between the calibrated $PM_{2.5}$ predicted by each of the non-linear equations versus the linear equation was 0.001 in each case. Because this difference is not meaningful, we decided to continue using linear equations for the rest of the analysis.

3.2 *Seasonality of* $PM_{2.5}$, *Delta-C, IR, and Delta-C:*$PM_{2.5}$

All season pairs of mean $PM_{2.5}$, Delta-C, IR, and Delta-C:$PM_{2.5}$ were statistically significantly different from each other ($p < 0.05$) except for: winter and summer fire Delta-C, spring and summer no fire Delta-C, spring and summer no fire IR, fall and summer no fire Delta-C:$PM_{2.5}$, spring and summer no fire Delta-C:$PM_{2.5}$, and fall and spring Delta-C:$PM_{2.5}$. Mean $PM_{2.5}$ concentrations were highest during the summer wildfire season, along with Delta-C and IR (Table 2). Delta-C:$PM_{2.5}$ was not highest during the summer wildfire season, possibly due to the combination of high $PM_{2.5}$ levels and decay of BrC in transported wildfire plumes (Forrister et al, 2015). Mean Delta-C was second highest in the winter, likely reflecting wintertime wood burning. The hourly mean wintertime Delta-C:$PM_{2.5}$ ratio in this study was 0.033, greater than the hourly mean ratios in the other seasons. Based on a period of high residential wood combustion during a winter inversion, Wang et al. identified a Delta-C:$PM_{2.5}$ ratio indicative of high contribution of wood smoke to $PM_{2.5}$ of 1:7.5 = 0.133 (Wang et al, 2011a), which is greater than the wintertime hourly mean ratio in this study but less than the maximum wintertime Delta-C:PM2.5 ratio in this study (0.27). Mean Delta-C:$PM_{2.5}$ in the fall was similar to spring and lower than winter at 0.011, while mean $PM_{2.5}$ was similar to winter. This suggests that there are other (non-BrC) important contributions to $PM_{2.5}$ in the fall.

Except for the summer wildfire smoke, these 9 months of sampling were relatively low for $PM_{2.5}$ for this area, especially in the winter (wintertime hourly mean was 7.7 μg/m^3, max 39 μg/m^3). In winter the year prior to this study (12/21/16-3/20/17) hourly mean was 16.9 μg/m^3, max 67 μg/m^3 (Washington State Department of Ecology). Overall trends for the county are available from Washington Tracking Network and report the following annual average 24-hour $PM_{2.5}$ from 2010 to 2016: 9.1, 10.2, 11.7, 12.9, 10.1, 13.3, and 11.6 μg/m^3 (Washington Tracking Network). Reduced wintertime $PM_{2.5}$ in this study compared to the previous year may be due to a combination of the success of the Yakama Nation Environmental Management Program's wood stove changeout program, and the sampled hours potentially capturing fewer than usual wintertime weather inversions and milder temperatures requiring less home heating.

Mean hourly Delta-C for the winter season was 0.27 μg/m^3, which is within the range of other reported wintertime mean Delta-C values in wood smoke impacted areas: 0.26 μg/m^3 in Laredo, TX (Wang et al, 2011b), and 0.10 to 0.34 μg/m^3 in Rochester, NY (Wang et al, 2011b; Wang et al, 2012c; Croft et al, 2017; Evans et al, 2017; Huang et al, 2011; Rich et al, 2018).

Author Manuscript Author Manuscript Author Manuscript Author Manuscript

Spring, fall, and summer without wildfire smoke hourly means of Delta-C ranged from 0.04 to 0.10, which is lower than most other reported means of Delta-C during non-winter seasons or year-round: −0.4 to 0.15 μg/m^3 in Rochester, NY (Wang et al, 2011b; Wang et al, 2012c; Wang et al, 2012a; Evans et al, 2017; Huang et al, 2011), and 0.21-1.58 μg/m^3 in Karachi, Pakistan (Malashock, 2012).

Summer wildfire smoke hourly mean and max of Delta-C (0.34 and 5.09) were lower than other reported Delta-C means during wildfire episodes: 20 and 8.0 μg/m^3 in Fort McMurray, Alberta (Landis et al, 2017). This may be due to previously mentioned decay of BrC in transported wildfire plumes (Forrister et al, 2015). The wildfire smoke impacting Yakima Valley originated from regional, not local, wildfires.

3.2.1 Use of Delta-C—Reports of the reliability of Delta-C to indicate wood smoke vary. Delta-C was found to be impacted by traffic emissions (Su et al, 2015), industrial emissions (Cheng et al, 2014), coal combustion (Kirchstetter et al, 2004; Olson et al, 2015), and other aerosols (Kirchstetter et al, 2004; Zhang et al, 2017; Olson et al, 2015) in addition to wood smoke. Harrison et al found that Delta-C did not capture wood smoke as well as levoglucosan (2012).

However, Delta-C was found to reflect diurnal and seasonal patterns expected from residential wood burning (Wang et al, 2011a; Wang et al, 2012a; Sandradewi et al, 2008; Zhang et al, 2017; Sofowote et al, 2014; Crilley et al, 2015), be sensitive to smoke from forest fires (Wang et al, 2011a; Wang et al, 2010; Landis et al, 2017; Kimbrough et al, 2015), be sensitive to other biomass burning and fireworks (Wang et al, 2011b; Kirchstetter et al, 2004), and not be associated with vehicle exhaust (Wang et al, 2011a; Kirchstetter et al, 2004; Wang et al, 2012b) in other studies. Delta-C was also found to correlate with other wood smoke markers – levoglucosan and potassium (Wang et al, 2011a; Harrison et al, 2012; Kimbrough et al, 2015; Crilley et al, 2015), and to correlate with $PM_{2.5}$ in wood smoke dominated environments (Zhang et al, 2017). In one study, Wang et al attributed more than 72% of Delta-C to a wood combustion factor (2012a).

Because Delta-C is sensitive to many types of biomass burning, it cannot be used to distinguish residential wood smoke from other biomass burning in areas with multiple biomass burning sources. Zhang et al caution that Delta-C is only semi-quantitative and in general cannot be used to signify a particular amount of a compound (2017). At the same time, Delta-C:$PM_{2.5}$ may indicate the relative contribution of biomass burning to total $PM_{2.5}$ (Wang et al, 2011a), implying that higher Delta-C:$PM_{2.5}$ is expected during instances of greater biomass burning. This is consistent with our study observations in this region with known wood burning for wintertime heat.

3.3 Wavelength dependence and absorption Ångström exponents by season

The a value based on mean absorbance was highest in the winter at 1.5, followed by summer wildfire at 1.4, fall at 1.3, and spring and summer no wildfire at 1.2 (Table 3). The relative height of the curves in Figure 3 reflects relative mass of BC and BrC. Seasonal a values had wide 95% CI that overlapped in all seasons. The a values are all within the range of other studies' values for seasons with higher expected biomass burning (0.98-1.6) (Favez

Author Manuscript Author Manuscript Author Manuscript Author Manuscript

et al, 2009; Sandradewi et al, 2008; Soni et al, 2011) and aerosols dominated by traffic emissions, soot, and diesel (~1-1.5) (Kirchstetter et al, 2004), but barely approach the range of values expected from biomass burning based on constrained studies (1.6-2.8) (Kirchstetter et al, 2004; Sandradewi et al, 2008; Zotter et al, 2017).

The low end of the non-winter CIs (1.0-1.1) were within the range of other studies' values for seasons with lower expected biomass burning (0.64-1.1) (Sandradewi et al, 2008; Soni et al, 2011) as well as higher expected biomass, traffic emissions, soot, and diesel, but are higher than values attributed to a modern motor vehicle fleet (0.9) (Zotter et al, 2017). According to estimates from Garg et al, these mean values are more representative of flaming (<1.4) rather than smoldering (>2) combustion conditions (2015).

The seasonal differences in a values were statistically significant (p-value <0.0001). Rank of a values in summer wildfire and wintertime were significantly different from the other three seasons: fall, spring, and summer no wildfire (Table 4). Summer wildfire and winter were not significantly different from each other, and fall, spring, and summer no wildfire were not significantly different from each other. This suggests that the aerosols in wintertime and summer wildfire were more dominated by emissions from biomass burning relative to the other seasons.

3.3.1 Use of Ångström exponents—In general, a has been observed to increase with more biomass burning (Kirchstetter et al, 2004; Zotter et al, 2017; Sandradewi et al, 2008). Favez et al found an average a (370–950 nm) of 1.25 in wintertime in Paris, France which is highly impacted by wintertime wood smoke (2009). Sandradewi et al reported average a (370–950 nm) values of 1.6 in the winter in a Swiss alpine valley highly impacted by wood smoke, 1.1 in the summer in the same valley, and 2.8 for a wood fire conducted in a laboratory (2008). Kirchstetter et al reported a over wavelengths ranging from a minimum of 330-450 nm to a maximum of 700-1100 nm for 20 different aerosol samples, and found that in general motor vehicle dominated aerosols had values around 1, while biomass dominated aerosols had values around 2 (2004). Kirchstetter et al also summarized the a findings of previous studies, which also tended towards ~1-1.5 for motor vehicle, soot, and diesel, and towards ~1.6-2.4 for biomass burning (2004).

Aerosols with a variety of pollution sources may have a values that do not clearly distinguish between higher and lower biomass burning expected with seasonal changes. Over 2 years in Delhi, India, Soni et al found that a values were 0.64, 0.68, 0.84, and 1.16 during seasons with lower expected biomass burning, and 0.98, 1.02, 1.19, and 1.21 during seasons with higher expected biomass burning (2011). Zotter et al found through comparisons between aethalometer data and elemental carbon source apportionment that an optimal a for traffic emissions is 0.9 and for wood burning is 1.68 (2017), however these values are based on emissions from a modern car fleet and constrained conditions for residential wood combustion, so may not apply to more complex aerosols.

Garg et al conducted a study in Mohali, India comparing a seven wavelength aethalometer to a mass spectrometer looking at a variety of emissions, including traffic and burning of agricultural residue, leaf litter, and garbage (2015). They suggest that combustion efficiency

Author Manuscript Author Manuscript Author Manuscript Author Manuscript

impacts a more than fuel type, where flaming conditions lead to lower a values (<1.4) and smoldering conditions lead to higher a values (>2) (Garg et al, 2015). Garg et al note that where aerosols are impacted by a variety of sources with a variety of combustion efficiencies, a may not be useful in identifying sources (2015).

While differences in a between seasons were statistically significant, the CIs for our observed values were wide. This could be due to the mixture of emissions sources and combustion conditions present in this region, including field and crop residue burning, low-temperature diesel emissions, truck traffic, backyard burning, and wood burning. Even the period of summer wildfire smoke did not produce a mean a clearly associated with biomass burning. This could be related to smoke aerosol characteristics changing during transport from regional wildfires, and wildfire combustion conditions.

In future studies, it may be helpful to target sampling to specific emissions in this area. For example, the aethalometer could be placed in the middle of a residential area with heavy wood stove use, or in the center of a large orchard using diesel-powered orchard heaters, or in an area dominated by one type of crop where the same type of burning occurs around the same time. Comparing results from targeted sampling may shed light on the small seasonal differences observed in this study, with a mixture of emissions.

3.4 Peak $PM_{2.5}$ hours

Summer wildfire had the greatest percentage of sampled hours over 12 μg/m^3 (Table 5). There is no general guidance available to assess health impacts of varying concentrations of hourly $PM_{2.5}$; the US EPA Air Quality Index (AQI) assesses 24-hour $PM_{2.5}$, and differentiates between the “Good” and “Moderate” category at an approximate $PM_{2.5}$ cut-point of 12 μg/m^3. 59% (453) of the sampled hours during the summer wildfire season had $PM_{2.5}$ concentrations over 12 μg/m^3. The mean a for these peak hours was 1.6, higher than summer wildfire overall. Fall had a slightly higher percentage of sampled hours over 12 μg/m^3 compared to winter. The mean a for fall peak hours was 1.2, which is lower than for fall overall, and the mean a for winter peak hours was 1.6, which is higher than for winter overall. This suggests that contributions to peak $PM_{2.5}$ in the fall are more dominated by emissions associated with diesel and soot (or more flaming combustion conditions), and contributions to peak $PM_{2.5}$ in the winter are more dominated by biomass burning.

While wintertime wood burning receives a lot of attention from a public health perspective, it is important to note that for this sampling period, winter and fall had a similar percentage of hours with $PM_{2.5}$ >12 μg/m^3. This could be related to a relatively mild winter sampling period, but still merits consideration. Agricultural emissions coinciding with the fall season include crop residue burning and orchard heaters, and deserve attention in future studies. The wildfire smoke period had more than double the percentage of sampled hours with $PM_{2.5}$ >12 μg/m^3 compared to winter and fall, underscoring the public health urgency surrounding wildfire smoke in this region.

3.5 Diurnal and weekday vs. weekend patterns

Marked differences were observed in diurnal patterns between seasons (Figure 4). No diurnal patterns were observed during spring; in the winter, $PM_{2.5}$ and Delta-C tended to be

Author Manuscript Author Manuscript Author Manuscript Author Manuscript

lower during midday hours. The fall pattern was similar to winter for Delta-C, but weaker than winter for $PM_{2.5}$. During the summer wildfire, $PM_{2.5}$ diurnal patterns did not resemble any of the other seasons. Winter a were slightly lower but also more varied during midday hours, while fall a were lower in the mornings and higher but more varied in the afternoons. Summer without wildfire had highly varied a values.

Median and 3rd quartile Delta-C values were very similar between weekdays and weekends across seasons, with Delta-C slightly higher on weekdays during summer wildfire (SI Table 3). $PM_{2.5}$ concentrations were slightly higher on weekdays than weekends during summer wildfire, spring, and fall. In contrast, $PM_{2.5}$ concentrations were very similar between weekdays and weekends in the winter and summer no wildfire. a were very similar between weekdays and weekends in each season, but slightly higher on winter, spring, and summer wildfire weekends.

Delta-C and $PM_{2.5}$ followed expected diurnal patterns for wintertime wood burning, with higher levels at night and lower levels during the day; this is due to a combination of diurnal changes in the atmospheric boundary layer and likely increased burning for heat at night. Winter a values were relatively similar throughout the day, with lower values in the middle of the day, reflecting the pattern in Delta-C, although the midday a values are more varied. In the fall, $PM_{2.5}$ had a weaker diurnal pattern, but Delta-C had a stronger diurnal pattern, and the diurnal pattern in fall a suggests an emissions profile more dominated by biomass burning at night vs. during the day. In combination with the lower mean a value for fall $PM_{2.5}$ peaks (Table 5), this suggests that there are important contributors to fall $PM_{2.5}$ with either a fuel mix less dominated by biomass, or more flaming combustion conditions.

Weekend vs. weekday differences observed may be due to the proximity of the monitors to schools, potentially capturing school-related traffic, including school buses. This traffic is not present on the weekends, but is still present to some degree in the summer. The diurnal pattern expected from school-related traffic is difficult to distinguish from other potential emissions sources along with changes in the atmospheric boundary layer.

Expected diurnal and weekly patterns in this region are different from urban or other non-agricultural regions. In other places, heating-related emissions are expected to be greater at night and on the weekends, and most other emissions (usually traffic) are expected to be lower at night and on the weekends. In agricultural areas, work-related emissions may not necessarily be lower at night and on weekends, as agricultural activities follow the seasons and weather patterns more than a typical urban work schedule. Some emissions are more likely to occur at night, such as orchard heating.

3.6 Use of low-cost sensors for spatial comparisons in $PM_{2.5}$

The low-cost monitors allowed us to expand upon the single BAM site, and compare PM concentrations between Toppenish and Harrah. Seasonal $PM_{2.5}$ concentrations were very similar between Toppenish and Harrah (Table 6). The SD for both Harrah and the low-cost monitor in Toppenish were lower than the BAM SD, which reflects the impact of the calibration. Similarly, the maximum values are lower than those measured by the BAM. The contrast in peak $PM_{2.5}$ between the BAM and low-cost monitor in Harrah during the wildfire

Author Manuscript Author Manuscript Author Manuscript Author Manuscript

season suggest that this difference is due to the impact of the calibration rather than reflecting a true difference in maximum $PM_{2.5}$ concentrations.

Technical and site-based challenges resulting in missing data impacted both low-cost and traditional monitors. Missing aethalometer data is due to delayed filter cartridge changes or power loss. The low-cost monitor in Toppenish had missing data due to time stamp dysfunction, and the low-cost monitor in Harrah was not deployed until late winter, and then had power loss. Missing BAM data is due to instrument recalibration needs. One Plantower in each low-cost monitor failed over the course of the study period, highlighting the importance of having duplicate sensors.

Missing data from the low-cost monitor in Toppenish (Figure 1) explains some of its discrepancy from the BAM. The BAM did not report data for several weeks in the winter during which the low-cost monitor in Toppenish did report data, so it is useful to note that in the winter the low-cost monitor is very similar to the BAM. This suggests that despite the high missingness in the BAM in the winter, the data we do have is likely representative - we are likely not missing a major peak or trough in winter $PM_{2.5}$ concentration. Typically when using low-cost monitors, we look to more accurate instruments, such as a BAM, to validate the data. Therefore, it was a surprising benefit in this case to be able to use the low-cost monitor data to verify that the BAM winter data is likely representative of the season despite high missingness.

4. Conclusion

This study is one of the first to pair low-cost PM monitors with an aethalometer, and addresses BrC and BC in a rural, agricultural setting. 9 months of data over 4 seasons, including episodes of wildfire smoke from regional wildfires, allowed us to characterize differences in combustion sources by season. Biomass burning is suspected to be a major contributor to $PM_{2.5}$ in the wintertime, and year-round $PM_{2.5}$ comes from a variety of sources, mainly agricultural-related. Low-cost monitors calibrated through co-location with regulatory instruments were useful in extending spatial information on $PM_{2.5}$, but calibration resulted in less variance. Having two Plantowers in each monitor was important because 1 failed in each monitor over the study period. Wintertime diurnal patterns of Delta-C and $PM_{2.5}$ were consistent with residential wood smoke. Mean Ångström exponent α values were highest during peak $PM_{2.5}$ hours in the winter and during the wildfire season, compared to other seasons, consistent with literature suggestions that higher α values are associated with biomass burning. Of the seasonal peak $PM_{2.5}$ hours, mean Ångström exponent α values were lowest during fall. In this region, the greatest percentage of sampled hours per season with $PM_{2.5}$ >12 $\mu g/m^3$ occurred during the wildfire smoke period, and were very similar between fall and winter. These results suggest that biomass burning is an important contributor to $PM_{2.5}$ in the wintertime, and emissions associated with diesel and soot are important contributors in the fall; however the variety of emissions sources and combustion conditions present in this region may limit the utility of traditional interpretations of aethalometer data. Further understanding of how to interpret aethalometer data in regions with complex emissions would contribute to much-needed research in communities impacted by air pollution from agricultural and home and backyard burning.

Author Manuscript Author Manuscript Author Manuscript Author Manuscript

Supplementary Material

Refer to Web version on PubMed Central for supplementary material.

Acknowledgements

We thank the Yakama Nation Environmental Management Program for their collaboration in this study, the Washington Department of Ecology for providing air monitoring data, Amanda Gassett and the UW MESA team for providing the low-cost monitors, and Jeff Blair (AethLabs) for technical support and providing feedback on this article. We are grateful to Taylor Hendricksen (UW) for administrative support.

This work was supported by the US Environmental Protection Agency (STAR Grant #RD83618501, Air Pollution Monitoring for Communities). Co-location at the Seattle Beacon Hill site was supported by a grant from the National Institutes of Health NIEHS R56ES026528. The funding sources had no involvement in the conduct of research or preparation of this article.

References:

AgWeatherNet. Washington State University. Web. " AgWeatherNet Current Conditions Map". <https://weather.wsu.edu/> Accessed 12/2/19.

Chakrabarti B, Fine PM, Delfino R, & Sioutas C (2004). Performance evaluation of the active-flow personal DataRAM PM2. 5 mass monitor (Thermo Anderson pDR-1200) designed for continuous personal exposure measurements. Atmospheric Environment, 38(20), 3329–3340.

Cheng YH, Lin CC, Liu JJ, & Hsieh CJ (2014). Temporal characteristics of black carbon concentrations and its potential emission sources in a southern Taiwan industrial urban area. Environmental Science and Pollution Research, 21(5), 3744–3755. [PubMed: 24281684]

Crilley LR, Bloss WJ, Yin J, Beddows DC, Harrison RM, Allan JD, … & Prevot AS (2015). Sources and contributions of wood smoke during winter in London: assessing local and regional influences. Atmospheric chemistry and physics, 15(6), 3149–3171.

Croft DP, Cameron SJ, Morrell CN, Lowenstein CJ, Ling F, Zareba W, … & Evans KA (2017). Associations between ambient wood smoke and other particulate pollutants and biomarkers of systemic inflammation, coagulation and thrombosis in cardiac patients. Environmental research, 154, 352–361. [PubMed: 28167447]

Day DE, Malm WC, & Kreidenweis SM (2000). Aerosol light scattering measurements as a function of relative humidity. Journal of the Air & Waste Management Association, 50(5), 710–716. [PubMed: 10842935]

Dunn OJ (1964). Multiple comparisons using rank sums. Technometrics, 6(3), 241–252.

EPA. AirNow AQI Calculator. United States Environmental Protection Agency Accessed 3/27/19 from: https://airnow.gov/index.cfm?action=airnow.calculator.

Estrada RD, & Ownby DR (2017). Rural Asthma: Current Understanding of Prevalence, Patterns, and Interventions for Children and Adolescents. Current Allergy and Asthma Reports, 17(6), 37. [PubMed: 28484946]

Evans KA, Hopke PK, Utell MJ, Kane C, Thurston SW, Ling FS, … & Rich DQ (2017). Triggering of ST-elevation myocardial infarction by ambient wood smoke and other particulate and gaseous pollutants. Journal of Exposure Science and Environmental Epidemiology, 27(2), 198. [PubMed: 27072425]

Favez O, Cachier H, Sciare J, Sarda-Estève R, & Martinon L (2009). Evidence for a significant contribution of wood burning aerosols to PM2. 5 during the winter season in Paris, France. Atmospheric Environment, 43(22-23), 3640–3644.

Forrister H, Liu J, Scheuer E, Dibb J, Ziemba L, Thornhill KL, … & Campuzano-Jost P (2015). Evolution of brown carbon in wildfire plumes. Geophysical Research Letters, 42(11), 4623–4630.

Garg S, Chandra BP, Sinha V, Sarda-Esteve R, Gros V, & Sinha B (2015). Limitation of the use of the absorption angstrom exponent for source apportionment of equivalent black carbon: a case study from the North West Indo-Gangetic Plain. Environmental science & technology, 50(2), 814–824. [PubMed: 26655249]

Author Manuscript Author Manuscript Author Manuscript Author Manuscript

Hagler GS, Yelverton TL, Vedantham R, Hansen AD, & Turner JR (2011). Post-processing method to reduce noise while preserving high time resolution in aethalometer real-time black carbon data. Aerosol and Air Quality Resarch, 11(5), 539–546.

Harrison RM, Beddows DCS, Hu L, & Yin J (2012). Comparison of methods for evaluation of wood smoke and estimation of UK ambient concentrations. Atmospheric Chemistry and Physics, 12(17), 8271–8283.

Huang J, Hopke PK, Choi HD, Laing JR, Cui H, Zananski TJ, … & Holsen TM (2011). Mercury (Hg) emissions from domestic biomass combustion for space heating. Chemosphere, 84(11), 1694–1699. [PubMed: 21620435]

Jayaratne R, Liu X, Thai P, Dunbabin M, & Morawska L (2018). The influence of humidity on the performance of a low-cost air particle mass sensor and the effect of atmospheric fog. Atmospheric Measurement Techniques, 11(8), 4883–4890.

Kelly KE, Whitaker J, Petty A, Widmer C, Dybwad A, Sleeth D, … & Butterfield A (2017). Ambient and laboratory evaluation of a low-cost particulate matter sensor. Environmental Pollution, 221, 491–500. [PubMed: 28012666]

Kimbrough S, Hays M, Preston B, Vallero DA, & Hagler GS (2015). Episodic Impacts from California Wildfires Identified in Las Vegas Near-Road Air Quality Monitoring. Environmental science & technology, 50(1), 18–24. [PubMed: 26618236]

Kirchstetter TW, Novakov T, & Hobbs PV (2004). Evidence that the spectral dependence of light absorption by aerosols is affected by organic carbon. Journal of Geophysical Research: Atmospheres, 109(D21).

Kruskal WH, & Wallis WA (1952). Use of ranks in one-criterion variance analysis. Journal of the American statistical Association, 47(260), 583–621.

Landis MS, Edgerton ES, White EM, Wentworth GR, Sullivan AP, & Dillner AM (2017). The impact of the 2016 Fort McMurray Horse River Wildfire on ambient air pollution levels in the Athabasca Oil Sands Region, Alberta, Canada. Science of The Total Environment.

Laskin A, Laskin J, & Nizkorodov SA (2015). Chemistry of atmospheric brown carbon. Chemical reviews, 115(10), 4335–4382. [PubMed: 25716026]

Liu HY, Schneider P, Haugen R, & Vogt M (2019). Performance assessment of a low-cost PM2. 5 sensor for a near four-month period in Oslo, Norway. Atmosphere, 10(2), 41.

Malashock DA (2012). Short-term associations between PM2. 5, black carbon, Delta-C, and cardiovascular diseases in a large developing megacity. State University of New York at Albany.

Morawska L, Thai PK, Liu X, Asumadu-Sakyi A, Ayoko G, Bartonova A, … Williams R (2018, 7 1). Applications of low-cost sensing technologies for air quality monitoring and exposure assessment: How far have they gone? Environment International. Elsevier Ltd 10.1016/j.envint.2018.04.018

Noonan CW, & Balmes JR (2010). Biomass smoke exposures: Health outcomes measures and study design. Inhalation toxicology, 22(2), 108–112. [PubMed: 20044883]

Olson MR, Victoria Garcia M, Robinson MA, Van Rooy P, Dietenberger MA, Bergin M, & Schauer JJ (2015). Investigation of black and brown carbon multiple-wavelength-dependent light absorption from biomass and fossil fuel combustion source emissions. Journal of Geophysical Research: Atmospheres, 120(13), 6682–6697.

Pohlert T (2014). The Pairwise Multiple Comparison of Mean Ranks Package (PMCMR). R package. http://CRAN.R-project.org/package=PMCMR.

Pruitt G (2014). PM Advance Program Path Forward. Yakima Regional Clean Air Agency.

Rich DQ, Utell MJ, Croft DP, Thurston SW, Thevenet-Morrison K, Evans KA, … & Hopke PK (2018). Daily land use regression estimated woodsmoke and traffic pollution concentrations and the triggering of ST-elevation myocardial infarction: a case-crossover study. Air Quality, Atmosphere & Health, 11(2), 239–244.

Sandradewi J, Prévôt ASH, Weingartner E, Schmidhauser R, Gysel M, & Baltensperger U (2008). A study of wood burning and traffic aerosols in an Alpine valley using a multi-wavelength Aethalometer. Atmospheric Environment, 42(1), 101–112.

Sayahi T, Butterfield A, & Kelly KE (2019). Long-term field evaluation of the Plantower PMS low-cost particulate matter sensors. Environmental pollution, 245, 932–940. [PubMed: 30682749]

Author Manuscript Author Manuscript Author Manuscript Author Manuscript

Schulte J (2017). $PM_{2.5}$ and PM_{10} Beta Attenuation Monitor Operating Procedure. Washington State Department of Ecology Publication no. 17-02-005. <https://fortress.wa.gov/ecy/publications/documents/1702005.pdf> Accessed 8/22/19.

Sioutas C, Kim S, Chang M, Terrell LL, & Gong H Jr (2000). Field evaluation of a modified DataRAM MIE scattering monitor for real-time PM2. 5 mass concentration measurements. Atmospheric Environment, 34(28), 4829–4838.

Sofowote UM, Rastogi AK, Debosz J, & Hopke PK (2014). Advanced receptor modeling of near–real–time, ambient PM2. 5 and its associated components collected at an urban–industrial site in Toronto, Ontario. Atmospheric Pollution Research, 5(1), 13–23.

Soni K, Singh S, Bano T, Tanwar RS, & Nath S (2011). Wavelength dependence of the aerosol Angstrom exponent and its implications over Delhi, India. Aerosol Science and Technology, 45(12), 1488–1498.

Su JG, Hopke PK, Tian Y, Baldwin N, Thurston SW, Evans K, & Rich DQ (2015). Modeling particulate matter concentrations measured through mobile monitoring in a deletion/substitution/addition approach. Atmospheric Environment, 122, 477–483.

VanderSchelden G, Foy B, Herring C, Kaspari S, VanReken T, & Jobson B (2017). Contributions of wood smoke and vehicle emissions to ambient concentrations of volatile organic compounds and particulate matter during the Yakima wintertime nitrate study. Journal of Geophysical Research: Atmospheres, 122(3), 1871–1883.

Wang Y, Huang J, Zananski TJ, Hopke PK, & Holsen TM (2010). Impacts of the Canadian forest fires on atmospheric mercury and carbonaceous particles in northern New York. Environmental science & technology, 44(22), 8435–8440. [PubMed: 20979360]

Wang Y, Hopke PK, Rattigan OV, Xia X, Chalupa DC, & Utell MJ (2011a). Characterization of residential wood combustion particles using the two-wavelength aethalometer. Environmental science & technology, 45(17), 7387–7393. [PubMed: 21774488]

Wang Y, Hopke PK, Rattigan OV, & Zhu Y (2011b). Characterization of ambient black carbon and wood burning particles in two urban areas. Journal of Environmental Monitoring, 13(7), 1919–1926. [PubMed: 21607243]

Wang Y, Hopke PK, Xia X, Rattigan OV, Chalupa DC, & Utell MJ (2012a). Source apportionment of airborne particulate matter using inorganic and organic species as tracers. Atmospheric environment, 55, 525–532.

Wang Y, Hopke PK, Rattigan OV, Chalupa DC, & Utell MJ (2012b). Multiple-year black carbon measurements and source apportionment using Delta-C in Rochester, New York. Journal of the Air & Waste Management Association, 62(8), 880–887. [PubMed: 22916435]

Wang Y, Hopke PK, & Utell MJ (2012c). Urban-scale seasonal and spatial variability of ultrafine particle number concentrations (Supplementary Material). Water, Air, & Soil Pollution, 223(5), 2223–2235.

Washington State Department of Ecology's Air Monitoring Website. Web. "Washington's Air Monitoring Network". < https://fortress.wa.gov/ecy/enviwa/> Accessed 8/22/19.

Washington Tracking Network. Washington State Department of Health. Web. "$PM_{2.5}$ Air Quality". Data obtained from EPA's Air Quality System. <https://fortress.wa.gov/doh/wtn/WTNPortal/#!q0=124> Accessed 5/29/19.

Zhang KM, Allen G, Yang B, Chen G, Gu J, Schwab J, … & Rattigan O (2017). Joint measurements of PM 2. 5 and light-absorptive PM in woodsmoke-dominated ambient and plume environments. Atmospheric Chemistry and Physics, 17(18), 11441–11452.

Zheng T, Bergin MH, Johnson KK, Tripathi SN, Shirodkar S, Landis MS, … & Carlson DE (2018). Field evaluation of low-cost particulate matter sensors in high-and low-concentration environments. Atmospheric Measurement Techniques, 11(8), 4823–4846.

Zikova N, Masiol M, Chalupa DC, Rich DQ, Ferro AR, & Hopke PK (2017). Estimating hourly concentrations of $PM_{2.5}$ across a metropolitan area using low-cost particle monitors. Sensors (Switzerland), 17(8). 10.3390/s17081922

Zotter P, Herich H, Gysel M, El-Haddad I, Zhang Y, Močnik G, … & Prévôt AS (2017). Evaluation of the absorption Ångström exponents for traffic and wood burning in the Aethalometer-based source

apportionment using radiocarbon measurements of ambient aerosol. Atmospheric chemistry and physics, 17(6), 4229–4249.

Author Manuscript Author Manuscript Author Manuscript Author Manuscript

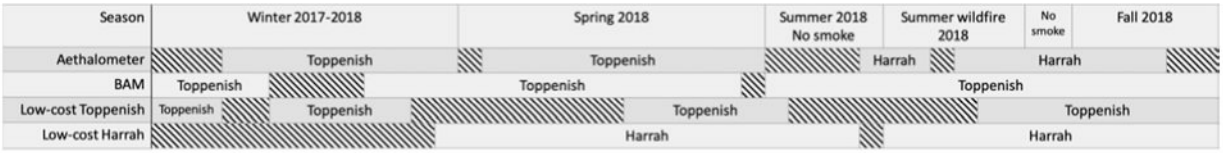

Figure 1:
Timeline of the study showing where and when monitors were running. Time periods with monitors not running are denoted by the diagonal lines.

Author Manuscript Author Manuscript Author Manuscript Author Manuscript

Author Manuscript Author Manuscript Author Manuscript Author Manuscript

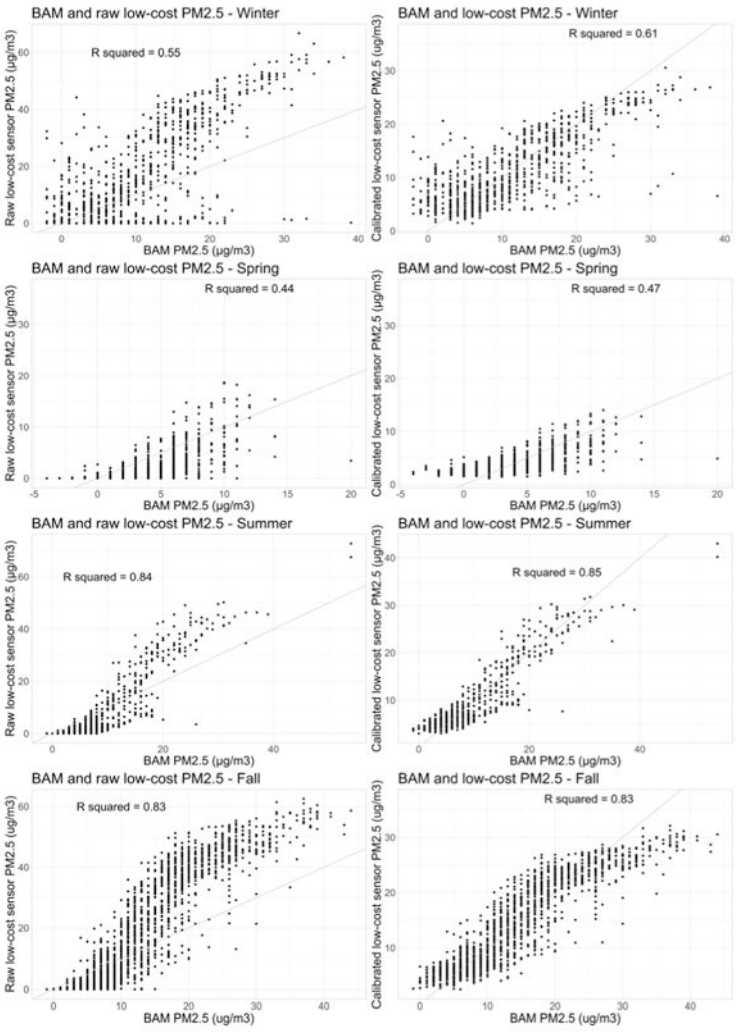

Figure 2:

Seasonal comparisons between raw low-cost and BAM $PM_{2.5}$ (µg/m^3) and calibrated low-cost and BAM $PM_{2.5}$ (µg/m^3) co-located in Toppenish.

Author Manuscript Author Manuscript Author Manuscript Author Manuscript

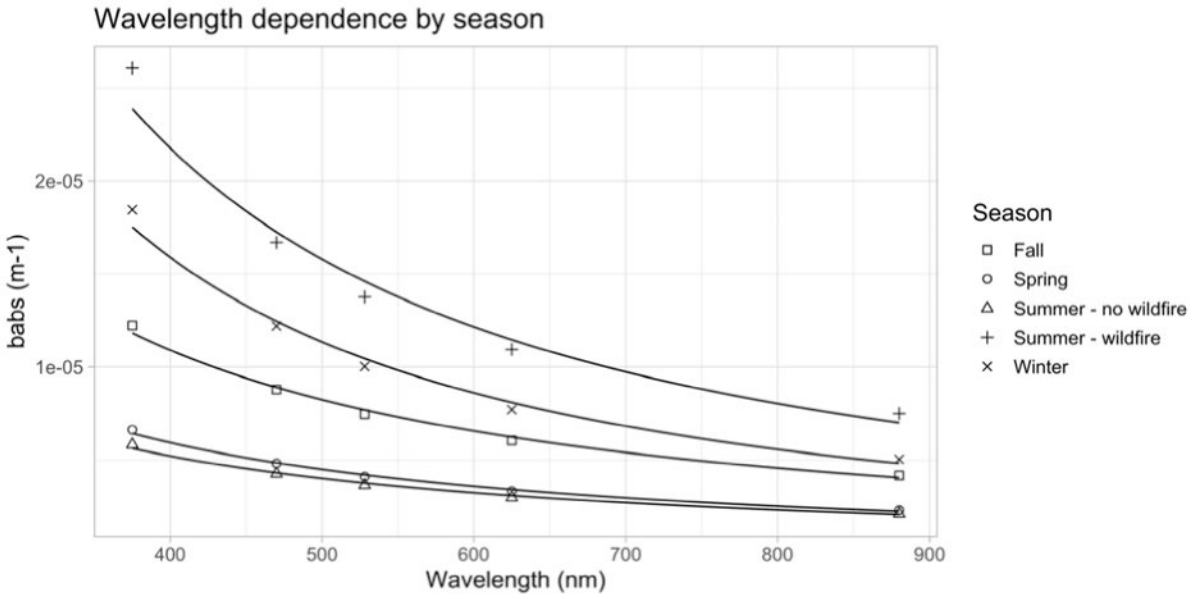

Figure 3:

Plot shows mean hourly absorption at each wavelength with power law curves for each season. Equations used for the curves are the following: winter $y = e^{-1.984} \times x^{-1.513}$, spring $y = e^{-4.600} \times x^{-1.241}$, summer wildfire $y = e^{-2.119} \times x^{-1.438}$, summer no wildfire $y = e^{-5.118} \times x^{-1.176}$, and fall $y = e^{-3.907} \times x^{-1.255}$.

Author Manuscript Author Manuscript Author Manuscript Author Manuscript

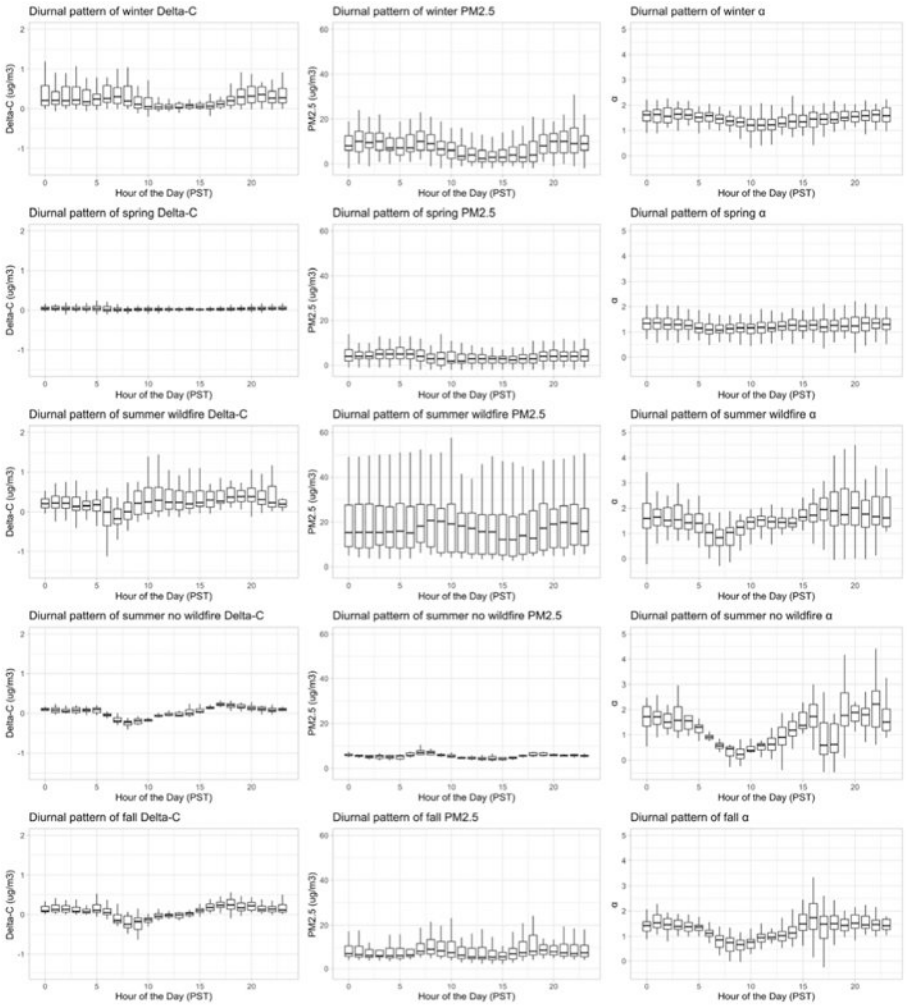

Figure 4:

Boxplots of Delta-C, $PM_{2.5}$, and Ångström exponent α values (375-880nm) per hour by season. Horizontal lines show the median value, boxes show the range from 1st quartile to 3rd quartile, and whiskers show 3rd quartile + 1.5 × interquartile range and 1st quartile – 1.5 × interquartile range. Each season has the same y-axis scale.

Author Manuscript

Author Manuscript

Author Manuscript

Author Manuscript

Table 1:

Seasonal hourly temperature and RH from co-located low-cost monitor and BAM, and nearby AgWeatherNet station in Toppenish. Only includes hours when all monitors are reporting.

	Winter Mean (SD) Range n=794 hours	**Spring Mean (SD) Range n=897 hours**	**Summer Mean (SD) Range n=694 hours**	**Fall Mean (SD) Range n=1504 hours**
BAM – Temperature (°C)	1.3 (4.9) −10.7 to 15.6	19.3 (5.2) 7.2 to 31.7	18.1 (5.4) 5.1 to 31.2	8.8 (7.1) −7.4 to 26.6
Low-cost monitor – Temperature (°C)	11.0 (4.4) 1.5 to 28.7	26.6 (7.3) 13.7 to 43.9	25.2 (7.4) 13.3 to 41.3	16.7 (6.6) 4.8 to 39.2
AgWeatherNet – RH (%)	81.4 (22.2) 23.8 to 99.6	49.6 (18.5) 14.8 to 99.2	53.4 (21.8) 16.8 to 94.1	72.7 (23.6) 16.6 to 99.7
Low-cost monitor - RH (%)	40.1 (7.9) 17.3 to 55.3	33.4 (12.2) 10.2 to 67.1	36.2 (12.9) 12.8 to 61.3	42.6 (11) 14.3 to 68.1

Author Manuscript Author Manuscript Author Manuscript Author Manuscript

Table 2:

Mean, standard deviation (SD), and range of temperature, RH, $PM_{2.5}$, Delta-C, mass at IR, and Delta-C:$PM_{2.5}$ by season for time periods with both $PM_{2.5}$ and co-located aethalometer data.

Temperature (°C) (BAM)	**Mean**	**SD**	**Min**	**Max**	**n hours**
Winter	5.3	4.1	−4.6	17.2	841
Spring	15.6	6.5	−0.2	31.7	1851
Summer – wildfire	22.2	6.0	9.7	38.1	794
Summer – no wildfire	19.4	7.9	5.1	37.7	431
Fall	12.2	5.6	0.8	26.6	690
RH (%) (AgWeatherNet)	**Mean**	**SD**	**Min**	**Max**	**n hours**
Winter	74.5	23.7	21.8	99.5	842
Spring	50.9	19.2	14.8	99.4	1851
Summer – wildfire	53.0	21.7	16.8	93.8	765
Summer – no wildfire	56.8	20.7	14.9	94.1	302
Fall	63.8	23.8	16.6	99.3	690
$PM_{2.5}$ (µg/m^3)	**Mean**	**SD**	**Min**	**Max**	**n hours**
Winter (BAM, Toppenish)	7.7	6.0	−4.0	39.0	843
Spring (BAM, Toppenish)	4.0	3.7	−4.0	43.0	1853
Summer – wildfire (BAM, Toppenish)	19.6	17.9	−1.0	95.0	794
Summer- wildfire (low-cost monitor, Harrah)	19.7	14.7	2.6	79.1	765
Summer – no wildfire (BAM, Toppenish)	8.8	4.9	0.0	26.0	432
Summer – no wildfire (low-cost monitor, Harrah)	5.8	1.8	3.0	16.5	302
Fall (BAM, Toppenish)	11.1	6.6	−1.0	43.0	687
Fall (low-cost monitor, Harrah)	9.1	5.2	2.2	24.8	691
Delta-C (µg/m^3)	**Mean**	**SD**	**Min**	**Max**	**n hours**
Winter	0.27	0.32	−0.25	2.76	843
Spring	0.048	0.11	−0.53	1.83	1853
Summer – wildfire	0.34	0.52	−1.48	5.09	765
Summer – no wildfire	0.035	0.14	−0.41	0.40	302
Fall	0.096	0.22	−0.63	2.07	691
Mass at IR (µg/m^3)	**Mean**	**SD**	**Min**	**Max**	**n hours**
Winter	0.50	0.42	−0.021	2.53	843
Spring	0.23	0.30	−0.035	6.13	1853
Summer – wildfire	0.74	0.84	−0.16	8.34	765
Summer – no wildfire	0.21	0.20	−0.16	0.96	302
Fall	0.41	0.38	−0.13	3.10	691

Note that $PM_{2.5}$ <1 µg/m3 were excluded when calculating Delta-C:$PM_{2.5}$.

Delta-C:$PM_{2.5}$	**Mean**	**SD**	**Min**	**Max**	**n hours**
Winter	0.033	0.034	−0.12	0.27	768
Spring	0.013	0.024	−0.075	0.37	1587
Summer – wildfire	0.017	0.023	−0.093	0.12	765
Summer – no wildfire	0.007	0.024	−0.060	0.060	302

Temperature (°C) (BAM)	Mean	SD	Min	Max	n hours
Fall	0.011	0.025	−0.079	0.17	691

Author Manuscript
Author Manuscript
Author Manuscript
Author Manuscript

Author Manuscript

Author Manuscript

Author Manuscript

Author Manuscript

Table 3:

Absorption Ångström exponents and 95% CI by season, based on linear regression on the log-log scale of the values shown in Figure 3.

Season	α (375-880) and 95% CI
Winter	1.5 (1.2-1.8)
Summer - wildfire	1.4 (1.0-1.8)
Fall	1.3 (1.1-1.4)
Spring	1.2 (1.1-1.4)
Summer – no wildfire	1.2 (1.0-1.3)

Author Manuscript

Author Manuscript

Author Manuscript

Author Manuscript

Table 4:

p-values from Dunn multiple comparison tests of rank of α values by season pairs.

	Spring	Summer – wildfire	Summer – no wildfire	Fall
Winter	<0.0001	0.66	<0.0001	<0.0001
Spring	--	<0.0001	1.00	0.08
Summer – wildfire	--	--	<0.0001	<0.0001
Summer – no wildfire	--	--	--	0.36

Author Manuscript

Author Manuscript

Author Manuscript

Author Manuscript

Table 5:

Number and percentage of sampled hours with $PM_{2.5}$ >12 μg/m^3 in each season and Ångström exponent α values and 95% CI based on mean absorbance at each wavelength during these peak hours.

Season	Number of hours per season with $PM_{2.5}$>12 μg/m^3	% of sampled hours per season with $PM_{2.5}$>12 μg/m^3	α(375-880) and 95% CI
Winter	179	21	1.6 (1.2-1.9)
Spring	40	2	1.4 (1.1-1.6)
Summer – wildfire	453	59	1.6 (1.0-1.8)
Summer – no wildfire	5	2	1.3 (1.3-1.5)
Fall	162	23	1.2 (1.0-1.5)

Author Manuscript Author Manuscript Author Manuscript Author Manuscript

Table 6:

Seasonal hourly $PM_{2.5}$ from the three monitors. Data shown from low-cost monitors are calibrated.

	Winter	**Spring**	**Summer no wildfire**	**Summer wildfire**	**Fall**
	$PM_{2.5}$ ($\mu g/m^3$)	**$PM_{2.5}$ ($\mu g/m^3$)**	**$PM_{2.5}$ ($\mu g/m^3$)**	**$PM_{2.5}$ ($\mu g/m^3$)**	**$PM_{2.5}$ ($\mu g/m^3$)**
	Mean (SD)	**Mean (SD)**	**Mean (SD)**	**Mean (SD)**	**Mean (SD)**
	Range	**Range**	**Range**	**Range**	**Range**
	n (hours)	**n (hours)**	**n (hours)**	**n (hours)**	**n (hours)**
BAM – Toppenish (all hours available)	10.1 (7.4) −4.0 to 39 n=1,365	4.1 (3.8) −4.0 to 43 n=1,912	7.1 (4.9) −2.0 to 50.0 n=1,108	27.1 (34.3) −1.0 to 272.0 n=954	13.9 (8.6) −1.0 to 44.0 n=1,649
Low-cost monitor – Toppenish (all hours available)	10.0 (5.8) 1.5 to 33.5 n=1,470	4.1 (2.2) 1.1 to 14.0 n=1,096	6.0 (1.8) 3.0 to 18.3 n=444	12.8 (8.1) 3.7 to 43.0 n=356	13.9 (7.9) 2.6 to 32.1 n=1,638
Low-cost monitor – Harrah (all hours available)	N/A	3.7 (2.8) −0.0 to 27.1 n=2,208	5.9 (2.3) 1.8 to 17.3 n=1,119	25.7 (25.2) 2.6 to 168.2 n=927	12.0 (7.3) 1.5 to 40.9 n=1,642
BAM – Toppenish (hours that coincide with the low-cost monitor in Toppenish)	11.5 (8.2) –2.0 to 39.0 n=794	4.0 (3.1) −4.0 to 20.0 n=898	6.2 (4.1) −1.0 to 26.0 n=340	12.6 (8.4) 0.0 to 54.0 n=354	13.9 (8.6) −1.0 to 44.0 n=1,638
Low-cost monitor – Toppenish (hours that coincide with the BAM)	11.5 (6.4) 1.4 to 30.6 n=794	4.0 (2.1) 1.1 to 14.0 n=898	6.1 (1.9) 3.0 to 18.3 n=340	12.7 (8.0) 3.7 to 43.0 n=354	13.9 (7.9) 2.6 to 32.1 n=1,638